Clim. Past Discuss., 8, 787–817, 2012
www.clim-past-discuss.net/8/787/2012/
doi:10.5194/cpd-8-787-2012

Climate of the Past Discussions

Madagascar corals reveal Pacific multidecadal modulation of rainfall since 1708

C. A. Grove[1], J. Zinke[1,2], F. Peeters[3], W. Park[4], T. Scheufen[1,5,*], S. Kasper[1], B. Randriamanantsoa[6], M. T. McCulloch[7], and G.-J. A. Brummer[1]

[1]NIOZ Royal Netherlands Institute for Sea Research, Department of Marine Geology, P.O. Box 59, 1790 AB Den Burg, Texel, The Netherlands
[2]The University of Western Australia and Oceans Institute, School of Earth and Environment, M004, Crawley, Western Australia 6009, Australia
[3]Vrije Universiteit Amsterdam, Faculty of Earth and Life Sciences, De Boelelaan 1105, 1081 HV Amsterdam, The Netherlands
[4]Helmholtz-Zentrum für Ozeanforschung Kiel (GEOMAR), Duesternbrooker Weg 20, 24105 Kiel, Germany
[5]University of Amsterdam, Institute for Biodiversity and Ecosystem Dynamics (IBED), Nieuwe Achtergracht 127, 1018 WS Amsterdam, The Netherlands
[6]Wildlife Conservation Society (WCS), B.P 8500 Soavimbahoaka, Antananarivo 101, Madagascar
[7]The University of Western Australia, School of Earth and Environment, M004 and ARC Centre of Excellence in Coral Studies, Crawley, Western Australia 6009, Australia

*now at: Unidad Académica de Sistemas Arrecifales, Instituto de Ciencias del Mar y Limnología, Universidad Nacional Autónoma de México, Apdo. Postal 1152, Cancún, Quintana Roo 77500, Mexico

Received: 15 February 2012 – Accepted: 1 March 2012 – Published: 12 March 2012

Correspondence to: C. A. Grove (craig.grove@nioz.nl)

Published by Copernicus Publications on behalf of the European Geosciences Union.

Abstract

The Pacific Ocean modulates Australian and North American rainfall variability on multidecadal timescales, in concert with the Pacific Decadal Oscillation (PDO). It has been suggested that Pacific decadal variability may also influence Indian Ocean surface temperature and rainfall in a far-field response, similar to the El Niño Southern Oscillation (ENSO) on interannual timescales. However, instrumental records of rainfall are too short and too sparse to confidently assess such multidecadal climatic teleconnections. Here, we present four climate archives spanning the past 300 yr from giant Madagascar corals. We decouple 20th century human deforestation effects from rainfall induced soil erosion using spectral luminescence scanning and geochemistry. The corals provide the first evidence for Pacific decadal modulation of rainfall over the Western Indian Ocean. We find that positive PDO phases are associated with increased Indian Ocean temperatures and rainfall in Eastern Madagascar, while precipitation in Southern Africa and Eastern Australia declines. Consequently, the negative PDO phase that started in 1998 should lead to reduced rainfall over Eastern Madagascar and increased precipitation in Southern Africa and Eastern Australia. We conclude that the PDO has important implications for future multidecadal variability of African rainfall, where water resource management is increasingly important under the warming climate.

1 Introduction

Tropical Indian Ocean warming in the 20th century has accelerated since the late 1970's affecting rainfall patterns and intensity across much of the Western Indian Ocean and adjacent landmasses of Eastern and Southern Africa (Richard et al., 2000; Funk et al., 2008). Warming of the South-Central Indian Ocean (0–15° S, 60–90° E) is thought to reduce the moisture flux towards sub-Saharan Africa promoting droughts in austral summer and fall (Goddard and Graham, 1999; Richard et al., 2000; Hoerling et al., 2006; Funk et al., 2008). As Eastern and Southern Africa heavily depends

CPD
8, 787–817, 2012

on regular rainfall for food production and ecosystem sustainability (Fleitmann et al., 2007), the uncertainty in the rainfall response to accelerated warming of the Indian Ocean is a serious socioeconomic issue of global importance (Funk et al., 2008). However, to fully assess this response it is necessary to identify the long-term natural rainfall patterns, yet currently we lack an understanding of the major drivers of natural decadal rainfall variability in the Indian Ocean and what the regional synergy is with global warming (Cane, 2010).

There is some evidence indicating that multidecadal South African rainfall is associated with ENSO-like interdecadal variability, due to the shifting tropical temperature troughs in response to large-scale changes in Indo-Pacific SST and sea level pressure (Reason and Rouault, 2002). Since rainfall patterns are sensitive to sea surface temperature (SST) change, which includes both natural internal variability and anthropogenic forcing, here we investigate natural multidecadal modulation of Indian Ocean rainfall in response to multidecadal SST variability. Massive corals such as *Porites* sp. generate precisely dated century-long, highly resolved and continuous proxy records of changing land-ocean interactions (Lough, 2007; McCulloch et al., 2003; Fleitmann et al., 2007). Here we present 300 yr of monthly resolved proxy records of soil erosion from four giant *Porites* sp. colonies growing in two coastal marine catchments of Eastern Madagascar (Fig. 1).

The PDO is a major internal mode of ocean-atmosphere variability (Mantua et al., 1997). Positive PDO phases are characterised by low SST in the Central Midlatitude Pacific and warm anomalies along the northern and eastern margins, and south of 30° N. The PDO is remotely forced from the Tropics in part (Schneider and Cornuelle, 2005), and responsible for strong multidecadal (50–70 yr) (Minobe, 1997) and interdecadal Pacific oscillations in SST (IPO; 17–28 yr) (Meehl and Hu, 2006). It is considered the leading mode of North Pacific SST defined by instrumental data for the past 120 yr (Mantua et al., 1997), and recognised in extended proxy time series, e.g. tree ring records of rainfall in NE Asia (D'Arrigo and Wilson, 2006). Moreover, mounting evidence indicates that the PDO has teleconnections extending over thousands of

CPD
8, 787–817, 2012

kilometers to the Indian Ocean (Cole et al., 2000; Crueger et al., 2009). The positive PDO phase corresponds to warm Indian Ocean SST anomalies (Deser et al., 2004), thought to exceed anomalies associated with ENSO (Krishnan and Sugi, 2003), particularly in the Southwestern Indian Ocean (Fig. 2a) (Meehl and Hu, 2006). While it is evident that changing rainfall patterns over Australia respond to the PDO (Arblaster et al., 2002), links to rainfall in Southeastern Africa and the Western Indian Ocean have only been suggested (Deser et al., 2004; Zinke et al., 2008).

2 Materials and methods

2.1 Coral sampling and analysis

Three corals MAS1, MAS3 and ANDRA were drilled in March 2007 from Antongil Bay, NE Madagascar, dating back to 1904, 1880 and 1914, respectively (Fig. 1) (Grove et al., 2010). The core MASB (15° 30,566 S; 49° 45,437 E) was drilled in October 2008, dating back to 1708. Three of the corals used for this study, MAS1, MAS3 and MASB are influenced by a major river draining into the Bay, named Antainambalana (Fig. 1). Its source lies 1450 m a.s.l. and its watershed covers an estimated 4000 km^2. As well as being influenced by the Antainambalana, a third coral ANDRA is located 30 km south of MAS1/3/B, and is influenced by a much smaller river called the Ambanizana, which has a watershed of 160 km^2.

The average growth rate of the three short coral cores was approximately 12 $mm\,y^{-1}$. Growth laminae were visualized by X-radiograph-positive prints, and the growth axis of the coral slab was defined as the line normal to these laminae. All cores were sectioned into 7 mm slabs, cleaned with sodium hypochlorite (NaOCl, 10–13 % reactive chloride; Sigma-Aldrich Company) for 24 h to remove residual organics that would quench luminescence, and subsequently scanned under UV-light to measure continuous spectral luminescence ratios (G/B). Luminescence in banded corals is indicative of past humic acid runoff from river discharge (Isdale, 1984; Barnes and Taylor, 2005; Lough et al.,

CPD
8, 787–817, 2012

2002; Grove et al., 2010). Indeed, correlations of MAS1 G/B and regional rainfall are statistically significant (Grove et al., 2010). Luminescence images of the MAS3 core revealed dark stains, likely organics, in the older sections of the core which could not be removed by bleaching, therefore as a precaution luminescence data ends in 1930.

Laser-Ablation Inductively Coupled Plasma Mass Spectrometry (Laser-Ablation ICP-MS) profiles were taken to analyse the trace element ratios of Sr/Ca, Ba/Ca and Mn/Ca at 40 µm intervals on the coral cores MAS1 and MAS3 at ANU Canberra (Sinclair et al., 1998; Fallon et al., 2002). Profiles cover the entire age of MAS1 (1906–2006) and since 1935 for MAS3 (1935–2006). We use Sr/Ca ratios as indicators of SST (Corrège, 2006; Alibert and McCulloch, 1997), whereas suspended sediment runoff is reconstructed using Ba/Ca ratios (Alibert and McCulloch, 1997; McCulloch et al., 2003; Sinclair and McCulloch, 2004). Ba/Ca in the coral cores analysed here showed a high temporal correlation with spectral luminescence ratios (Grove et al., 2010). Mn/Ca is used as an indicator of ash fallout from slash and burn deforestation (Abram et al., 2003; Lewis et al., 2007). As luminescence and Laser-Ablation data have a sub-weekly resolution, interpolation to a monthly time-series provides a high level of accuracy.

2.2 Research area and climate setting

Coral cores were taken from Antongil Bay in NE Madagascar, which is surrounded by one of the country's largest remaining rainforests (Birkinshaw and Randrianjanahary, 2007). Air temperature and rainfall in Antongil Bay was monitored for the period 1992 to 1996 (Kremen, 2003). Antongil Bay is characterised by an August–December cold-dry season and a January–July warm-wet season. Air temperatures peak in December and January and are lowest between July and September. Highest rainfall occurs between January and April, while lowest rainfall occurs between September and November (Kremen, 2003; Jury et al., 1995). The annual average precipitation at Andranobe (coral site ANDRA) was 6049 mm (1 SD = 979 mm) between 1992 and 1996. Highest river discharge occurs between February and April, one to two months after

CPD
8, 787–817, 2012
Madagascar corals reveal Pacific multidecadal modulation of rainfall
C. A. Grove et al.

peak rainfall (Gerten et al., 2008). Runoff decreases but continues until September then reaches lows in October and November.

3 Results and discussion

We measured soil-derived humic acids in the coral skeletons by spectral luminescence scanning (Green/Blue ratio; G/B) to determine seasonally resolved runoff resulting from hinterland rainfall (Grove et al., 2010). Our longest coral G/B record dating from 1708 to 2008 (MASB; Fig. 1) was compared to the NE Asia tree ring based PDO reconstruction (D'Arrigo and Wilson, 2006) to investigate multidecadal variability in rainfall (Fig. 2a, grey box), since the instrumental PDO index (Mantua et al., 1997) only dates back to 1880. Both climate records show near identical changes in amplitude and timing for over two centuries (Fig. 1c) then diverge after the 1920's. Cross spectral (Fig. 3) and wavelet coherence analysis (Fig. 4) of the PDO tree ring index and MASB G/B confirm the clear relationship between rainfall and the PDO on multidecadal time scales since at least 1708 and until the 1920's (Appendix A). Coherent temporal changes in signal amplitudes and timing between both records show that positive phases of the PDO correspond to positive rainfall anomalies (Fig. 2c).

To further investigate post 1920 PDO modulation of Eastern Madagascar soil runoff, we also analysed the G/B records of additional corals in combination with high resolution geochemistry. We used Laser-Ablation ICP-MS to determine coral Ba/Ca as a proxy of past sediment runoff (McCulloch et al., 2003; Fleitmann et al., 2007), Sr/Ca as a robust proxy for SST (Abram et al., 2003; Zinke et al., 2008) and Mn/Ca as an indicator for ash fallout from slash and burn deforestation (Abram et al., 2003; Lewis et al., 2007). Together, they allowed us to decouple the three major components influencing Eastern Madagascar soil runoff; i.e. human land-use changes and natural decadal climate variability interacting with Indian Ocean warming. Long-term changes in runoff appear in the 10-yr running mean of both G/B and Ba/Ca in each coral (MAS1, Fig. 5a,c; MAS3, Fig. 5d,f). Most pronounced is the continuous increase in humic acid runoff since the mid-1970s and sediment runoff from the mid-1950s, towards a maximum in recent years in concert with rising South Central Indian Ocean SST (Fig. 5). Also, the longest continuous precipitation record from Madagascar (Antananarivo) is in agreement with our Ba/Ca and SST records, whereby rainfall increased from the mid-1950s until the record ends in 1987 (Fig. 5b,e). Consequently, increasing rainfall (runoff) over the catchment area appears tightly coupled to rising SST (Fig. 5).

The reduced coherence between humic acid runoff and Indian Ocean SST in the mid-20th century suggests that other factors are involved in large-scale erosion. Discrepancies between 1945–1955 and 1966–1980 occur in both cores whereby G/B increases while temperature decreases (1940–1960) or remains stable (1960–1980). These periods are also marked by enhanced coral Mn/Ca above the seasonal background (Figs. 5 and B1; Appendix B), as found in response to ash fallout from wild fires (Abram et al., 2003; Lewis et al., 2007). Indeed, the pronounced increase in Mn/Ca testifies to the well documented intense slash-and-burn deforestation for upland rice cultivation between 1950 and 1980 (Green and Sussman, 1990; Harper et al., 2007), associated with the economic collapse of Madagascar and the return to subsistence agriculture. Segmentation analysis (Webster, 1973, 1979) of the coral composite G/B record (MAS1, MAS3 and ANDRA) highlights these mid-20th century human deforestation periods (Figs. C1 and C2; Appendix C; see Supplement).

The coupling between increasing runoff and Central Indian Ocean warming is evident after the prominent climate shift around 1976/77 when both global mean temperatures and rainfall strongly increased (Fig. 5) (Meehl et al., 2009). As Mn is also associated with seasonal soil runoff through erosion (Lewis et al., 2007), we observe similar increasing linear trends in the G/B and Mn/Ca ratios in response to Indian Ocean warming (Fig. B1; Appendix B). As G/B is a direct indicator of soil erosion and not rainfall, we removed the deforestation effect from the record prior to spectral analysis and filtering of the MAS1 time series by subtracting the normalised record of Mn/Ca from the normalised G/B record (Figs. 6 and B1; Appendix B). This also removed the long-term erosion trend, resulting in a G/B-Mn/Ca record that is reflecting the natural rainfall

CPD
8, 787–817, 2012

variability, now increasing from the mid-1950s in agreement with the SST and Ba/Ca data (Figs. 5 and 6).

Spectral analysis of the monthly instrumental PDO index (1880-present) (Mantua et al., 1997) and coral G/B-Mn/Ca show strong power in the multidecadal band (Fig. B2), in agreement with the pre-1920 frequency analysis of MASB G/B and the tree ring based PDO index (Figs. 3 and 4). The tight temporal relationship with the PDO index shows that a positive (negative) phase is associated with wet (dry) conditions (Fig. 6). Interestingly, G/B-Mn/Ca correlates with typical positive PDO-like conditions in global SSTs, coupled with a positive correlation with South Central Indian Ocean SST (Fig. 6). Also, in the Sr/Ca temperature proxy record of MAS1, a positive PDO phase is associated with a warm SST anomaly (Fig. 7), pointing to a typical response to Pacific decadal forcing found in Indian Ocean SST (Krishnan and Sugi, 2003; Cole et al., 2000; Deser et al., 2004; Crueger et al., 2009). The temporal alignment of all records (Sr/Ca, Ba/Ca, G/B-Mn/Ca) with the PDO (Fig. 7) therefore argue for Pacific modulation of Madagascar rainfall on multidecadal timescales for at least the past 300 yr.

Madagascar is an iconic example of the extreme environmental impacts human deforestation and habitat destruction has on soil runoff and land degradation (Green and Sussman, 1990; Harper et al., 2007). Human activity is also reported for two 200–300 yr erosion records from Kenya that show a simultaneous major shift in base level runoff at 1906 ± 3 yr and 1908 ± 5 yr (Fleitmann et al., 2007). This 1908 shift in soil erosion was attributed predominantly to a change from traditional subsistence agriculture to intensive European land-use practices introduced by the British settlers. Yet, the Kenya coral records also indicate accelerated soil erosion between the late 1940s and early 1950s and in the late 1970s following periods of intense drought which occur simultaneously with shifts in our Madagascar coral records. These multidecadal runoff changes co-occur with the 1905, 1947 and 1976 shifts in the PDO, also suggesting a Pacific modulation of Kenyan soil erosion by rainfall.

The PDO/river runoff relationship in Great Barrier Reef corals and East Australia river gauges is opposite to that in Madagascar, as the negative PDO phase (i.e. 1947 to 1976) is linked with higher river discharge, and vice versa, for the positive PDO phase (Lough, 2007; McGowan et al., 2009). Correlating precipitation with the principle component time series of the IPO (Meehl and Hu, 2006), and the PDO (Felis et al., 2010) shows a negative response over Eastern Australia and Southern Africa, and a positive response in Eastern Madagascar and Eastern Africa (Fig. D1; Appendix D). Since Indian Ocean SST is sensitive to the PDO (Krishnan and Sugi, 2003) and rainfall is linked to SST (Goddard and Graham, 1999), runoff variability is ultimately controlled by Pacific Ocean multidecadal variability. During the positive PDO phase, higher mean SST is responsible for enhanced atmospheric convection over the Indian Ocean, which in turn drives anomalous subsidence over Southern Africa and Eastern Australia (Lough, 2007; Goddard and Graham, 1999; Richard et al., 2000; Hoerling et al., 2006; McGowan et al., 2009).

Long term coral data provide the first evidence that Southwest Indian Ocean rainfall is linked to the PDO on multidecadal time scales. Consequently, for the upcoming decades rainfall in Eastern Madagascar should decrease as the PDO is currently in a transition from a positive to a negative phase. Elsewhere, PDO teleconnected regions with weaker rains in recent decades should experience more precipitation, i.e. in Eastern Australia and Southern Africa. However, it remains a major milestone in future research to unravel if and when projected anthropogenic warming of the Indian Ocean (Forster et al., 2007) will dominate rainfall over the inherent multidecadal component. Our data illustrate this interplay as an acceleration of rainfall and erosion following the prominent 1976/77 climate shift (Meehl et al., 2009), which is related to both anthropogenic and multidecadal forcing. The widespread operation of Pacific multi-decadal modulation recognised here provides new constraints for future rainfall patterns on human timescales that will assist in water management, soil conservation and biodiversity programmes throughout the tropical Indo-Pacific.

CPD
8, 787–817, 2012

Appendix A

Coherence and wavelet analysis

We compared the long time series of the PDO and MASB directly without using an agent (CIO SST). Annual mean data of the PDO reconstruction (D'Arrigo and Wilson, 2006) and MASB for the period 1708–1920 were used for coherence analysis. The reconstructed PDO (D'Arrigo and Wilson, 2006) and MASB show significant power at decadal, interdecadal and centennial time scales (Fig. 3a, b). Strong coherence between the PDO and MASB is found at multidecadal (60 yr) and bidecadal (15–30 yr) frequencies, with the PDO slightly leading MASB (Fig. 3c). Further, wavelet coherence analysis (Grinsted et al., 2004) with the same time series supports strong coherence between the PDO and MASB on interannual, bidecadal (20–30 yr) and multidecadal bands (Fig. 4).

Appendix B

Coral Mn/Ca

The MAS1 Mn/Ca record is in and out of phase with the MAS1 G/B time-series on seasonal timescales (Fig. B1). This indicates that high Mn concentrations, associated with slash and burn deforestation, are likely flushed into Antongil Bay during both the wet and dry seasons. Both the G/B and Mn/Ca have similar runoff trends as shown by their linear equations (Fig. B1). This indicates that a fraction of Mn is flushed into the bay associated with the soils or sediment, not just ash fallout (Lewis et al., 2007). This fraction is, however, far weaker in concentration than that associated with ash fallout (Abram et al., 2003). By subtracting the normalised Mn/Ca record from the normalised G/B record, we remove the deforestation effect, as well as the long-term runoff trend (Fig. B1), leaving a G/B-Mn/Ca record that shows the natural runoff variability (Figs. 6

CPD
8, 787–817, 2012

and B2). This method is conceptually similar to removing the thermal component of coral skeletal $\delta^{18}O$ by subtracting Sr/Ca, leaving the salinity component $\delta^{18}O_{sw}$ (Ren et al., 2002).

Appendix C

Record segmentation analysis

Record segmentation analysis of the coral composite G/B record, which includes MAS1, MAS3 and ANDRA (Fig. 1), identify years within the G/B time series that correspond to phase changes in the PDO, South Central Indian Ocean SST and periods of major deforestation (Figs. C1 and C2; see Supplement). Two major shifts are detected in the PDO time series: in 1944 and 1976. The timing of these major shifts is in agreement with PDO multi-decadal changes as described in previous studies (Minobe, 1997; Mantua et al., 1997). The 1944 shift of the PDO is associated with a shift in our composite G/B record (Fig. C1); however, SST data shows a highly significant transition 2 yr later in 1946 (Fig. C2). This is most likely an artefact created by the sampling bias in observational data for this period (Gedalof et al., 2002). At the second major shift in the PDO in 1976, the South Central Indian Ocean SST shows a prolonged transition from 1976 to 1982, whereas the G/B records a sharper transition in 1982 (Fig. C1). This difference in the timing of the transition is likely a perturbation created by the 1970s deforestation period. The transitions in G/B associated with the years surrounding 1955–1958 and 1970 (Figs. C1 and C2) are assigned to the enhanced deforestation marked by the highly pronounced Mn/Ca peaks (Fig. 2; Fig. B1). As the record segmentation method uses 2 × 10 yr windows, the 1970's deforestation period influences the timing of the defined G/B transition (1982) in relation to the 1976 PDO shift.

Significant shifts (2 × 10 yr window) in the G/B also occurred in 1921–1925, 1930, 1944, 1955–1958, 1970, 1982, 1987–1988 and recently in 1994 (Figs. C1 and C2).

CPD
8, 787–817, 2012

Other than the two major shifts in the PDO (Mantua et al., 1997; Gedalof et al., 2002) at 1944 and 1976 (1982), significant transitions at 1921–1925, 1930–1933, 1957, 1989 and 1994 also co-occur with G/B (Fig. C1). The south CIO SST shows transitions in 1918, 1946, 1957, 1976–1982, 1987 and 1994–1997 (Fig. C2). Minor shifts in the PDO are associated with the interdecadal frequency mode (Interdecadal Pacific Oscillation/IPO), which are also recorded in the G/B and the south CIO SST at 1921–1925, 1930–1933, 1955–1958, 1987–1989 and 1994 (Figs. C1 and C2). The 1994 shift most likely marks the start of a transition to a negative PDO phase on multi-decadal time scales (Verdon and Franks, 2006). The deforestation period in the 1950's overlaps with one of the interdecadal changes in the PDO and south CIO SST.

Appendix D

Spatial correlation of the PDO with rainfall

A spatial correlation of the PDO and global rainfall supports our results, with a negative correlation shown in Southern Africa, Eastern Australia (Lough, 2007; McGowan et al., 2009) and the Northern Rocky Mountains (St. Jacques et al., 2010), as well as a positive correlation in Madagascar (Fig. D1). These results are replicated by the spatial correlation pattern of the IPO (Meehl and Hu, 2006) and PDO (Felis et al., 2010) with precipitation.

Supplementary material related to this article is available online at: http://www.clim-past-discuss.net/8/787/2012/cpd-8-787-2012-supplement.pdf.

Acknowledgements. This work was supported as part of the SINDOCOM grant under the Dutch NWO program "Climate Variability", grant 854.00034/035. Additional support comes from the NWO ALW project CLIMATCH, grant 820.01.009, and the Western Indian Ocean Marine Science Association through the Marine Science for Management programme under grant MASMA/CC/2010/02. We thank the Wildlife Conservation Society (WCS) Madagasacar, especially Heriliala Randriamahazo and the WCS/ANGAP team in Maroantsetra, for their support in fieldwork logistics and in the organisation of the research permits. We would also like to thank CAF/CORE Madagascar for granting the CITES permit and ANGAP Madagascar for support of our research activities in the vicinity of the marine and forest nature parks. Furthermore, we would like to thank Bob Koster and Rineke Gieles for their continuous development and maintenance of the XRF-Core Scanner, and Rik Tjallingii and Thomas Richter for their fruitful discussions concerning the manuscript. We are grateful to the ARC Centre of Excellence in Coral Reef Studies and ANU Research School of Earth Sciences for support of the Laser-Ablation analysis.

References

Abram, N. J., Gagan, M. K., McCulloch, M. T., Chappell, J., and Hantoro, W. S.: Coral reef death during the 1997 Indian Ocean Dipole linked to Indonesian wildfires, Science, 301, 952–955, 2003.

Alibert, C. and McCulloch, M. T.: Strontium/calcium ratios in modern Porites corals from the Great Barrier Reef as a proxy for sea surface temperature: calibration of the thermometer and monitoring of ENSO, Paleoceanography, 12, 345–363, 1997.

Arblaster, J. M., Meehl, G. A., and Moore, A.: Interdecadal modulation of Australian rainfall, Clim. Dynam., 18, 519–531, 2002.

Barnes, D. J. and Taylor, R. B.: On the nature and causes of luminescent lines and bands in coral skeletons: II. Contribution of skeletal crystals, J. Exp. Mar. Biol. Ecol, 322, 135–142, 2005.

Birkinshaw, C. and Randrianjanahary, M.: The effects of Cyclone Hudah on the forest of Masoala Peninsula, Madagascar, Madagascar Conserv. Dev., 2, 17–20, 2007.

Cane, M. A.: Decadal predictions in demand, Nat. Geoscie., 3, 231–232, 2010.

Cole, J. E., Dunbar, R. B., McClanahan, T. R., and Muthiga, N. A.: Tropical Pacific forcing of decadal SST variability in the Western Indian Ocean over the past two centuries, Science, 287, 617–619, 2000.

Corrège, T.: Sea surface temperature and salinity reconstructions from coral geochemical tracers, Palaeogeogr. Palaeoclimatol. Palaeoecol., 232, 408–428, 2006.

Crueger, T., Zinke, J., and Pfeiffer, M.: Patterns of Pacific decadal variability recorded by Indian Ocean corals, Int. J. Earth Sci., 98, 41–52, 2009.
D'Arrigo, R. and Wilson, R.: On the Asian expression of the PDO, Int. J. Climatol., 26, 1607–1617, 2006.
Deser, C., Phillips, A. S., and Hurrell, J. W.: Pacific interdecadal climate variability: linkages between the tropics and the North Pacific during boreal winter since 1900, J. Climate, 17, 3109–3124, 2004.
Fallon, S. J., White, J. C., and Mcculloch, M. T.: Porites corals as recorders of mining and environmental impacts: Misima Island, Papua New Guinea, Geochim. Cosmochim. Ac., 66, 45–62, 2002.
Felis, T., Suzuki, A., Kuhnert, H., Rimbu, N., and Kawahata, H.: Pacific decadal oscillation documented in a coral record of North Pacific winter temperature since 1873, Geophys. Res. Lett., 37, L14605, doi:10.1029/2010GL043572, 2010.
Fleitmann, D., Dunbar, R. B., McCulloch, M. T., Mudelsee, M., Vuille, M., McClanahan, T. R., Cole, J. E., and Eggins, S.: East African soil erosion recorded in a 300 year old coral colony from Kenya, Geophys. Res. Lett., 34, L04401, doi:10.1029/2006GL028525, 2007.
Forster, P., Ramaswamy, V., Artaxo, P., Berntsen, T., Betts, R., Fahey, D. W., Haywood, J., Lean, J., Lowe, D. C., Myhre, G., Nganga, J., Prinn, R., Raga, G., Schulz, M., and Van Dorland, R.: Changes in atmospheric constituents and in radiative forcing, Chapt. 2, in: Climate Change 2007: The Physical Science Basis. Contribution of Working Group I to the Fourth Assessment Report of the Intergovernmental Panel on Climate Change, edited by: Solomon, S., Qin, D., Manning, M., Chen, Z., Marquis, M., Averyt, K. B., Tignor, M., and Miller., H. L., Cambridge Univ. Press, Cambridge, UK, 2007.
Funk, C., Dettinger, M. D., Michaelsen, J. C., Verdin, J. P., Brown, M. E., Barlow, M., and Hoell, A.: Warming of the Indian Ocean threatens Eastern and Southern African food security but could be mitigated by agricultural development, P. Natl. Acad. Sci. USA, 105, 11081–11086, 2008.
Gedalof, Z., Mantua, N. J., and Peterson, D. L.: A multi-century perspective of variability in the Pacific Decadal Oscillation: new insights from tree rings and coral, Geophys. Res. Lett., 29, 2204, doi:10.1029/2002GL015824, 2002.
Gerten, D., Rost, S., von Bloh, W., and Lucht, W.: Causes of change in 20th century global river discharge, Geophys. Res. Lett., 35, L20405, doi:10.1029/2008GL035258, 2008.

CPD
8, 787–817, 2012

Goddard, L. and Graham, N. E.: Importance of the Indian Ocean for simulating rainfall anomalies over Eastern and Southern Africa, J. Geophys. Res., 104, 19099–19116, 1999.
Green, G. M. and Sussman, R. W.: Deforestation history of the eastern rain forests of Madagascar from satellite images, Science, 248, 212–215, 1990.
Grinsted, A., Moore, J. C., and Jevrejeva, S.: Application of the cross wavelet transform and wavelet coherence to geophysical time series, Nonlinear Proc. Geoph., 11, 561–566, 2004.
Grove, C. A., Nagtegaal, R., Zinke, J., Scheufen, T., Koster, B., Kasper, S., McCulloch, M. T., van den Bergh, G., and Brummer, G-J. A.: River runoff reconstructions from novel spectral luminescence scanning of massive coral skeletons, Coral Reefs, 29, 579–591, 2010.
Harper, G. J., Steininger, M. K., Tucker, C. J., Juhn, D., and Hawkins, F.: Fifty years of deforestation and forest fragmentation in Madagascar, Environ. Conserv., 34, 325–33, 2007.
Hoerling, M., Hurrell, J., Eischaid, J., and Phillips, A.: Detection and attribution of 20th century Northern and Southern African rainfall change, J. Climate, 19, 3989–4008, 2006.
Isdale, P.: Fluorescent bands in massive corals record centuries of coastal rainfall, Nature, 310, 578–579, 1984.
Jury, M. R., Parker, B. A., Raholijao, N., and Nassor, A.: Variability of summer rainfall over Madagascar: climate determinants at interannual scales, Int. J. Climatol., 15, 1323–1332, 1995.
Kremen, C.: The Masoala Peninsula, in: The Natural History of Madagascar: the Masoala Peninsula, edited by: Goodman, S. M. and Benstead J. P., University of Chicago Press, Chicago, 1459–1466, 2003.
Krishnan, P. and Sugi, M.: Pacific decadal Oscillation and variability of the Indian summer monsoon rainfall, Clim. Dyn., 21, 233–242, 2003.
Lewis, S. L., Shields, G. A., Kamber, B. S., and Lough, J. M.: A multi-trace element coral record of land-use changes in the Burdekin River catchment, NE Australia, Palaeogeogr. Palaeoclimatol. Palaeoecol., 246, 471–487, 2007.
Lough, J. M.: Tropical river flow and rainfall reconstructions from coral luminescence: Great Barrier Reef, Australia, Paleoceanography, 22, PA2218, doi:10.1029/2006PA001377, 2007.
Lough, J. M., Barnes, D. J., and Mcallister, F. A.: Luminescent lines in corals from the Great Barrier Reef provide spatial and temporal records of reefs affected by land runoff, Coral Reefs, 21, 333–343, 2002.
Mantua, N. J., Hare, S. R., Zhang, Y., Wallace, J. M., and Francis, R. C.: A Pacific interdecadal climate oscillation with impacts on salmon production, B. Am. Meteorol. Soc., 78, 1069–1079,

1997.
McCulloch, M. T., Fallon, S., Wyndham, T., Hendy, E., Lough, J., and Barnes, D.: Coral record of increased sediment flux to the inner Great Barrier Reef since European settlement, Nature, 421, 727–730, 2003.
McGowan, H. A., Marx, S. K., Denholm, J., Soderholm, J., and Kamber, B. S.: Reconstructing annual inflows to the headwater catchments of the Murray River, Australia, using the Pacific Decadal Oscillation, Geophys. Res. Lett., 36, L06707, doi:10.1029/2008GL037049, 2009.
Meehl, G. A. and Hu, A.: Megadroughts in the Indian monsoon region and Southwest North America and a mechanism for associated Multidecadal Pacific Sea Surface Temperature Anomolies, J. Climate, 19, 1605–1623, 2006.
Meehl, G. A., Hu, A., and Santer, B. D.: The mid-1970s climate shift in the Pacific and the relative roles of forced versus inherent decadal variability, J. Climate, 22, 780–792, 2009.
Minobe, S.: A 50–70 year climatic oscillation over the North Pacific and North America, Geophys. Res. Lett., 24, 683–686, doi:10.1029/97GL00504, 1997.
Mitchell, T. D. and Jones, P. D.: An improved method of constructing a database of monthly climate observations and associated high-resolution grids, Int. J. Climatol., 25, 693–712, doi:10.1002/joc.1181, 2005.
Reason, C. J. C. and Rouault, M.: ENSO-like decadal variability and South African rainfall, Geophys. Res. Lett., 29, 1638–1641, doi:10.1029/2002GL014663, 2002.
Ren, L., Linsley, B. K., Wellington, G. M., Schrag, D. P., and Hoegh-Guldberg, O.: Deconvolving the δ^{18}O seawater component from subseasonal coral δ^{18}O and Sr/Ca at Rarotonga in the Southwestern Subtropical Pacific for the period 1726 to 1997, Geochim. Cosmochim. Ac., 67, 1609–1621, 2002.
Richard, Y., Trzaska, S., Roucou, P., and Rouault, M.: Modification of the Southern African rainfall variability/ENSO relationship since the late 1960's, Clim. Dynam., 16, 883–895, 2000.
Schneider, N. and Cornuelle, B. D.: The forcing of the Pacific Decadal Oscillation, J. Climate, 18, 4355–4373, 2005.
Sinclair, D. J. and Mcculloch, M. T.: Corals record low mobile barium concentrations in the Burdekin River during the 1974 flood: evidence for limited Ba supply to rivers?, Palaeogeogr. Palaeoclimatol. Palaeoecol., 214, 155–174, 2004.
Sinclair, D. J., Kinsley, L. P. J., and Mcculloch, M. T.: High resolution analysis of trace elements in corals by laser ablation ICP-MS, Geochim. Cosmochim. Ac., 62, 1889–1901, 1998.

Smith, T. M., Reynolds, R. W., Peterson, T. C., and Lawrimore, J.: Improvements to NOAA's historical merged land-ocean surface temperature analysis (1880–2006), J. Climate, 21, 2283–2296, 2008.

St. Jacques, J.-M., Sauchyn, D. J., and Zhao, Y.: Northern Rocky Mountain streamflow records: global warming trends, human impacts or natural variability?, Geophys. Res. Lett. 37, L06407, doi:10.1029/2009GL042045, 2010.

Verdon, D. C. and Franks, S. W.: Long-term behaviour of ENSO: interactions with the PDO over the past 400 years inferred from paleoclimate records, Geophys. Res. Lett., 33, L06712, doi:10.1029/2005GL025052, 2006.

Webster, R.: Automatic soil-boundary location from transect data, Math. Geol., 5, 27–37, 1973.

Webster, R.: Divide: a FORTRAN IV program for segmenting multivariate one-dimensional spatial series, Comput. Geosci., 6, 61–68, 1979.

Zinke, J., Pfeiffer, M., Timm, O., Dullo, W.-C., Kroon, D., and Thomassin, B. A.: Mayotte coral reveals hydrological changes in the Western Indian Ocean between 1881 and 1994, Geophys. Res. Lett., 35, L23707, doi:10.1029/2008GL035634, 2008.

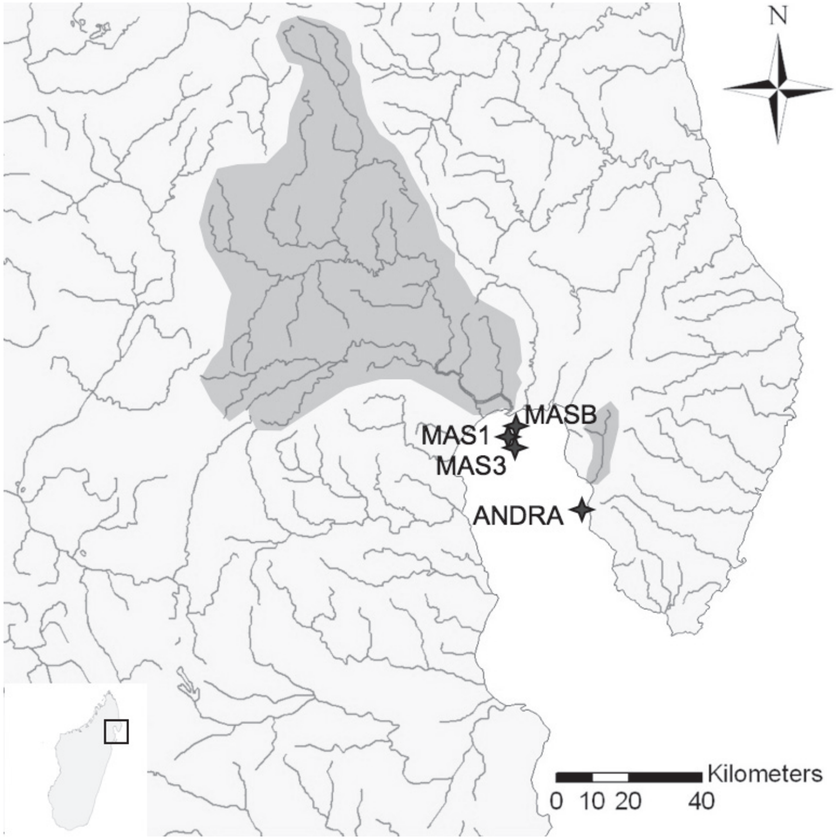

Fig. 1. Map of the region where cores MAS1, MAS3, MASB and ANDRA were drilled. Coral locations (stars) and their corresponding rivers and watersheds (grey shaded areas) are marked accordingly in Antongil Bay. The largest river is the Antainambalana, influencing MAS1, MAS3 and MASB; the river influencing ANDRA is the Ambanizana, flowing south westward into the bay.

CPD
8, 787–817, 2012

Madagascar corals reveal Pacific multidecadal modulation of rainfall

C. A. Grove et al.

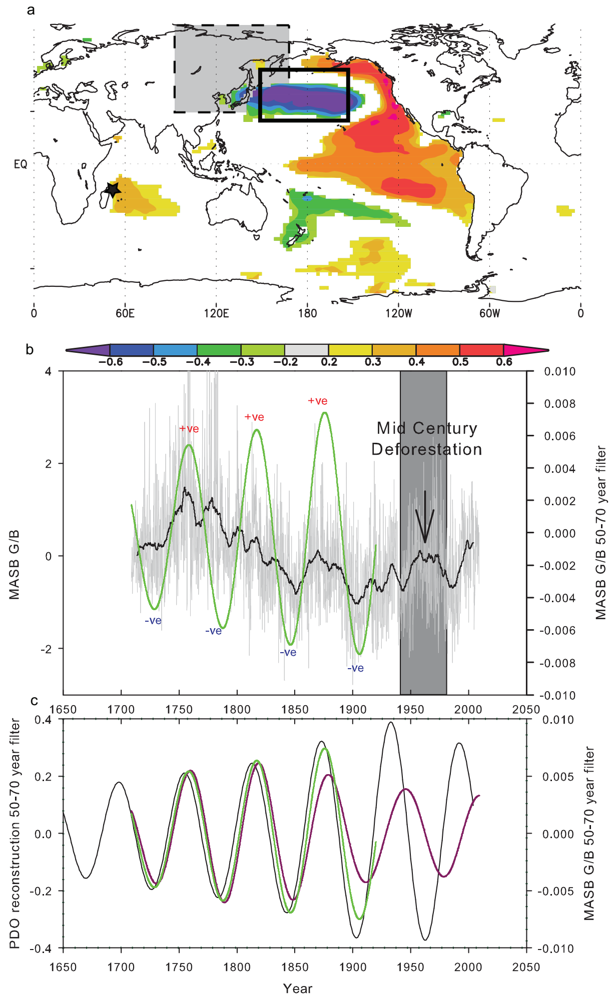

Fig. 2. Caption on next page.

CPD

8, 787–817, 2012

Madagascar corals reveal Pacific multidecadal modulation of rainfall

C. A. Grove et al.

Fig. 2. Typical positive PDO phase **(a)** indicated by global SST anomalies. Yearly (January–December) global SST (ERSSTv.3) correlate with the PDO index (Mantua et al., 1997), with positive and negative anomalies at $>90\,\%$ significance level indicated by colours. The black outlined box on the map **(a)** shows the strong negative anomalies of the Central North Pacific during a positive PDO phase. The grey shaded box **(a)** indicates the region used to compile the NE Asian 500 yr reconstructed tree ring PDO index (D'Arrigo and Wilson, 2006). Monthly MASB G/B (grey line) and the 10 yr running mean (black line) are shown **(b)** together with the 50–70 yr band-pass filtered (0.017000 ± 0.002800) data up to 1920 (green). Peaks and troughs **(b)** represent multidecadal positive (red) and negative (blue) runoff anomalies. The same 50–70 yr band pass filter **(c)** is also applied to the tree ring based PDO reconstruction (black), MASB G/B 1708–2008 (purple) and MASB G/B 1708–1920 (green). Both the tree ring based PDO reconstruction and the MASB G/B 1708–1920 are coherent **(c)**, therefore positive PDO phases are associated with positive runoff anomalies. When considering the total MASB G/B time series (1708–2008), the relationship with the reconstructed PDO index breaks down post 1920.

CPD
8, 787–817, 2012

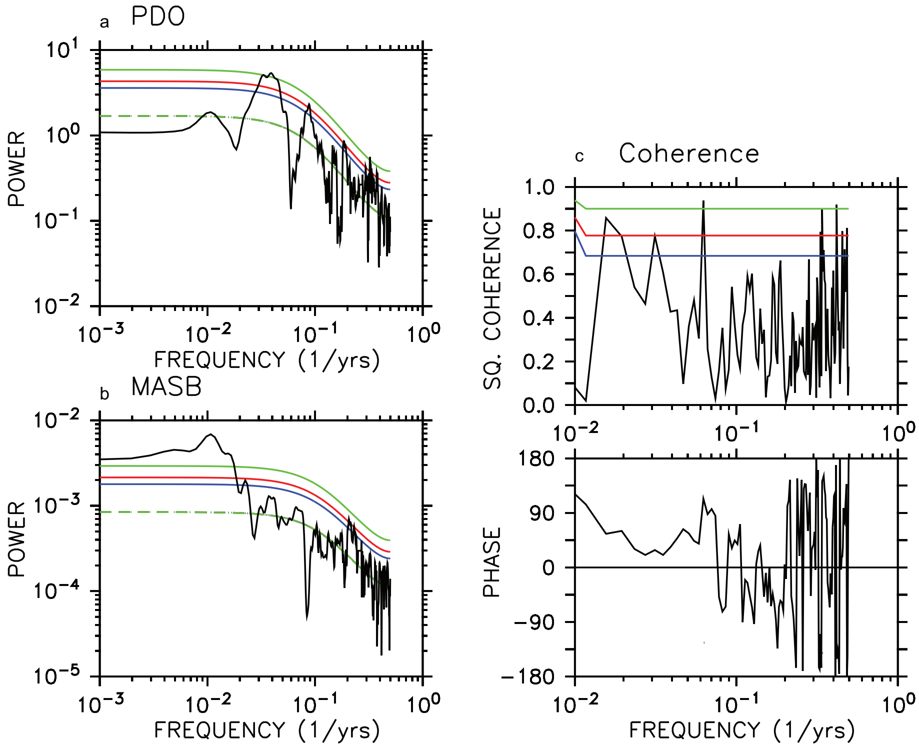

Fig. 3. Spectrum of **(a)** the tree ring based PDO reconstruction (D'Arrigo and Wilson, 2006) and **(b)** MASB. Annual mean data are used for the analysis during 1708–1920 when two data sets are commonly available. Confidence levels are indicated with green (99 %), red (95 %), blue (90 %) and green dashed (median) lines, respectively. Coherence and phase lag of the two annual datasets **(c)** are shown. Positive phase lag represents the lead of the PDO. Data are detrended prior to the analysis.

CPD
8, 787–817, 2012

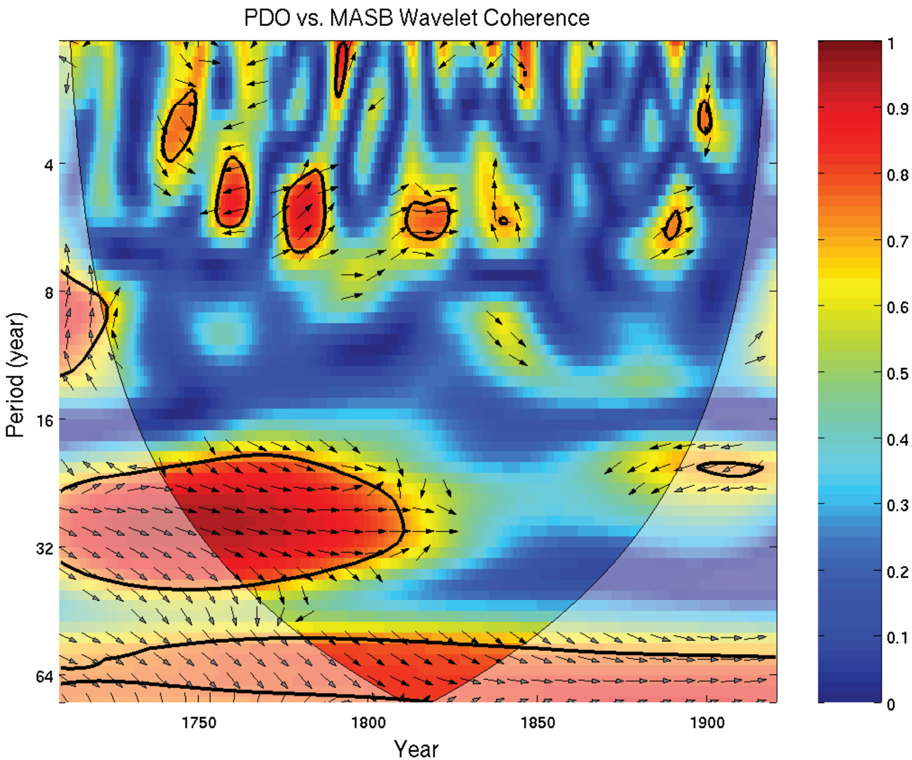

Fig. 4. Cross wavelet coherence analysis with the tree ring based PDO reconstruction (D'Arrigo and Wilson, 2006) and MASB G/B indices, as used in Fig. 3. The 5 % significance level against red noise is shown as a thick contour. Phases are indicated as arrows, where directing right represents an in phase, and a clockwise direction indicates a lead of the PDO.

CPD
8, 787–817, 2012

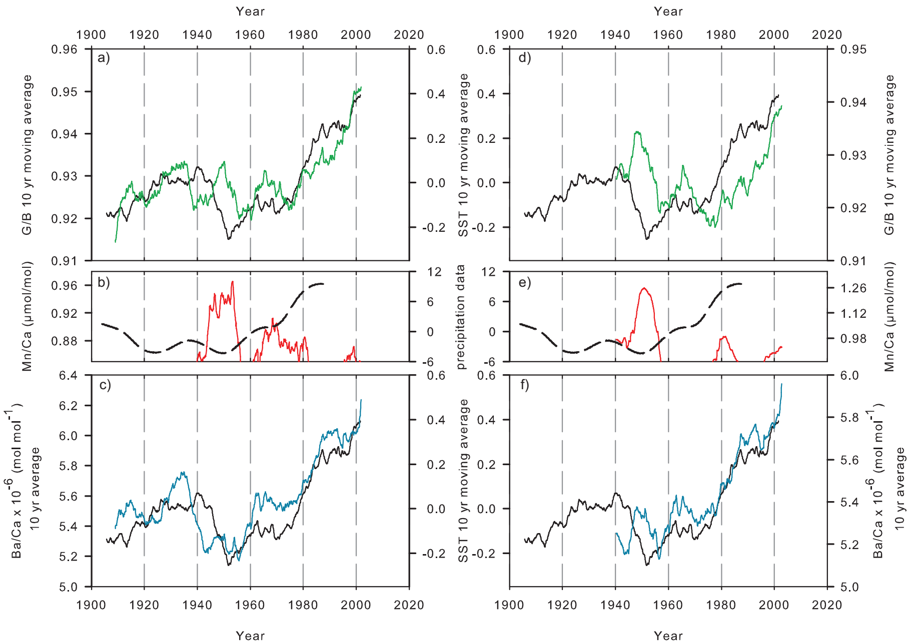

Fig. 5. A 10 yr running mean of MAS1 and MAS3 coral G/B (green) compared to the SST anomaly (ERSSTv.3) for the Southern Central Indian Ocean 5–20° S, 60–90° E (black) since 1904 **(a, d)**, the coral Mn/Ca (red solid; µmol mol) **(b, e)**, and the Ba/Ca (blue) **(c, f)**. Note that multi-decadal oscillations in G/B and Ba/Ca show high coherence with SST. Higher Mn/Ca ratios identify periods of slash and burn deforestation that overprint the climatic control of humic acid runoff. Differences observed between Ba/Ca and G/B is linked to watershed composition. A 120 month low pass filter of Antananarivo precipitation anomalies (18.80° S, 47.50° E, 1276 m, WMO station code: 67083 ANTANANARIVO/IVATO) is shown (black dashed; **b, e**), indicating increasing rainfall conditions. Note that this precipitation record ends in 1987 due to recent data gaps.

CPD
8, 787–817, 2012

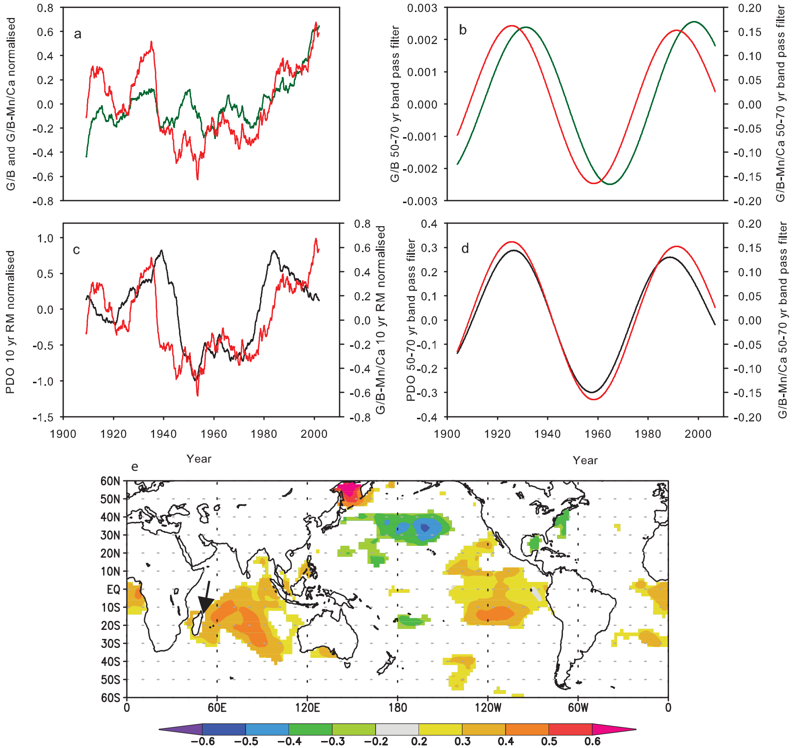

Fig. 6. The 10 yr running means **(a, c)** and 50–70 yr band pass filter (**b, d**; 0.017000 ± 0.002800) of normalised MAS1 G/B (green), normalised MAS1 G/B-Mn/Ca (red) and the PDO (black). Note, with the removal of Mn/Ca from the G/B record, runoff is now in phase with the PDO. The spatial correlation of global SST (ERSSTv.3) with **(e)** the 360-month low pass filter of normalised MAS1 G/B-Mn/Ca is shown, indicating PDO-like spatial SST patterns (Fig. 2a). Only correlations above 90 % significance level are shown. Correlations were computed at http://climexp.knmi.nl/. An arrow points the region where all coral cores were drilled in NE Madagascar.

CPD
8, 787–817, 2012

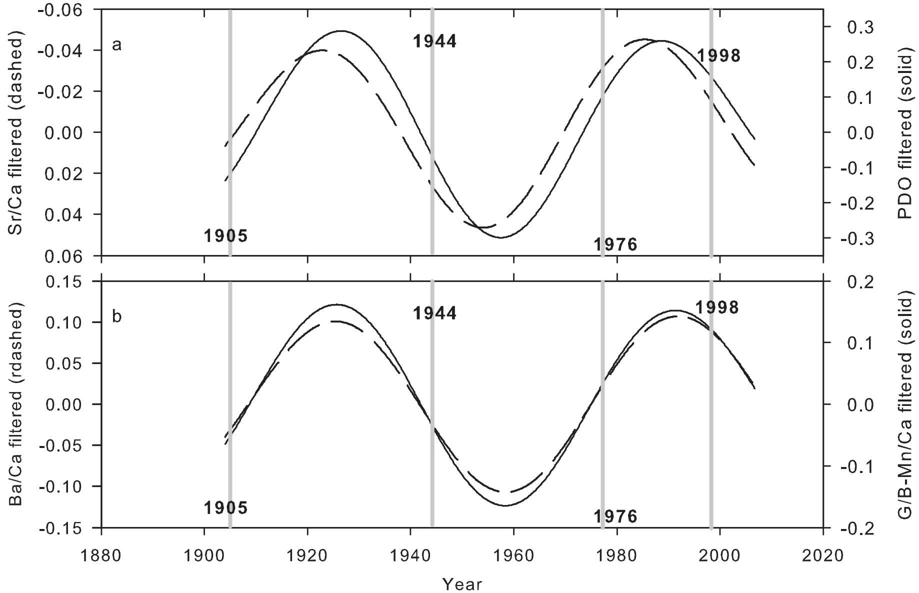

Fig. 7. A 50–70 yr band pass filter (0.017000 ± 0.002800) applied to **(a)** the MAS1 Sr/Ca data (dashed) and the Mantua PDO index (solid); and **(b)** MAS1 Ba/Ca (dashed) and MAS1 G/B-Mn/Ca (solid). The grey bars represent the transition years of different phase changes of the PDO.

CPD
8, 787–817, 2012

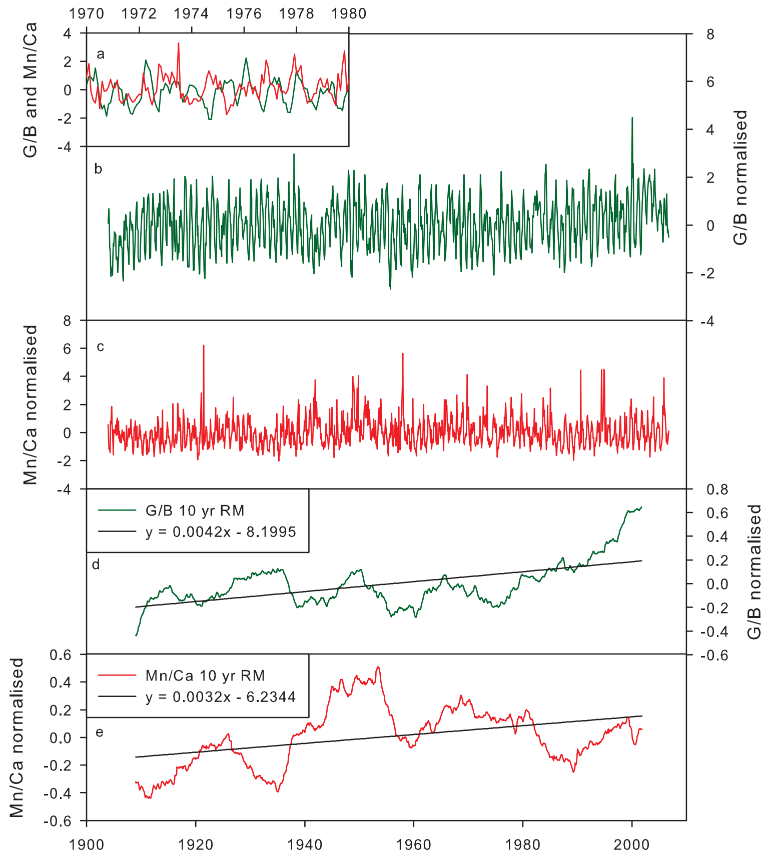

Fig. B1. The seasonal alignment of **(a)** the MAS1 coral G/B record with Mn/Ca values for the years 1970–1980. The complete time-series of normalised **(b)** G/B and **(c)** Mn/Ca is shown in green and red, respectively. The 10 yr running means of **(d)** G/B and **(e)** Mn/Ca are shown together with linear trends (black line). The regression equations of each line are given in the top left hand corner of each plot. Note that the trend lines have a similar slope.

CPD
8, 787–817, 2012

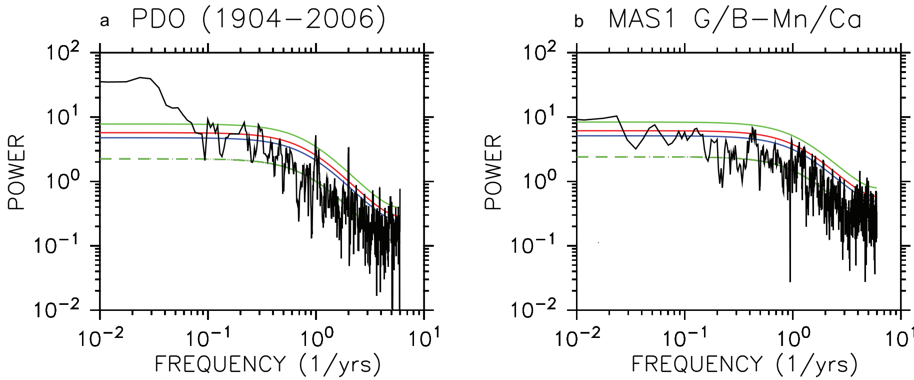

Fig. B2. Spectrum of **(a)** the PDO index (Mantua et al., 1997) and **(b)** MAS1 G/B-Mn/Ca. Monthly anomaly data from January 1904 to October 2006 are used, whereby the monthly climatology of 1971–2000 is removed. Detrended data are standardised prior to spectral analysis. Confidence levels are indicated with green (99 %), red (95 %), blue (90 %) and green dashed (median) lines, respectively.

CPD
8, 787–817, 2012

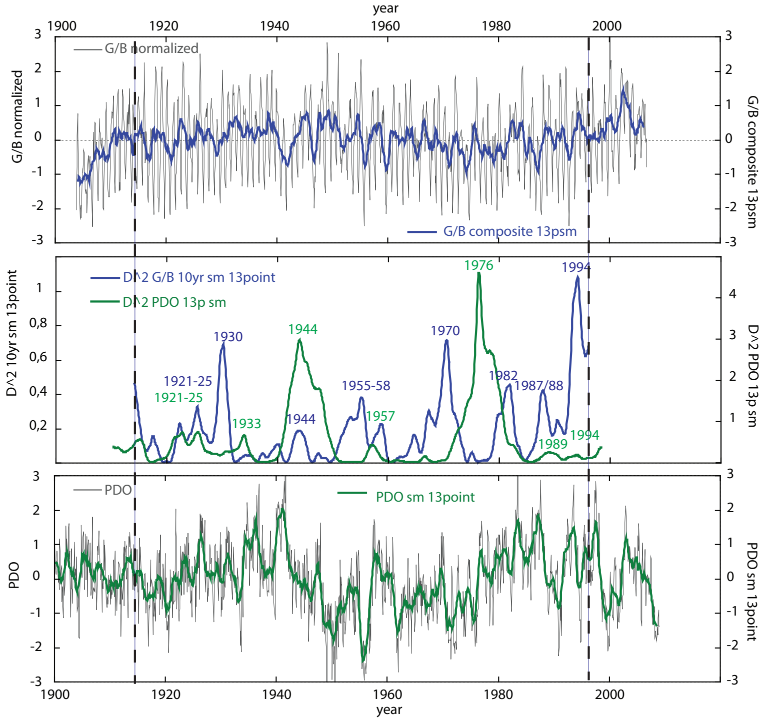

Fig. C1. Record segmentation of the PDO vs. 3 core composite G/B (MAS1, MAS3 and ANDRA). The top panel shows the raw G/B record with a 13 point smoothing superimposed. Middle Panel shows the change points which are above the 95 % significance level. Major change points are indicated by years (green = PDO; blue = G/B). Lower panel shows the raw PDO time series with a 13 point smoothing superimposed. The vertical dashed line marks the start and end point for reliable interpretation of the record segmentation analysis taking into account that the first and last 10 yr cannot be used for interpretation.

CPD
8, 787–817, 2012

Madagascar corals reveal Pacific multidecadal modulation of rainfall

C. A. Grove et al.

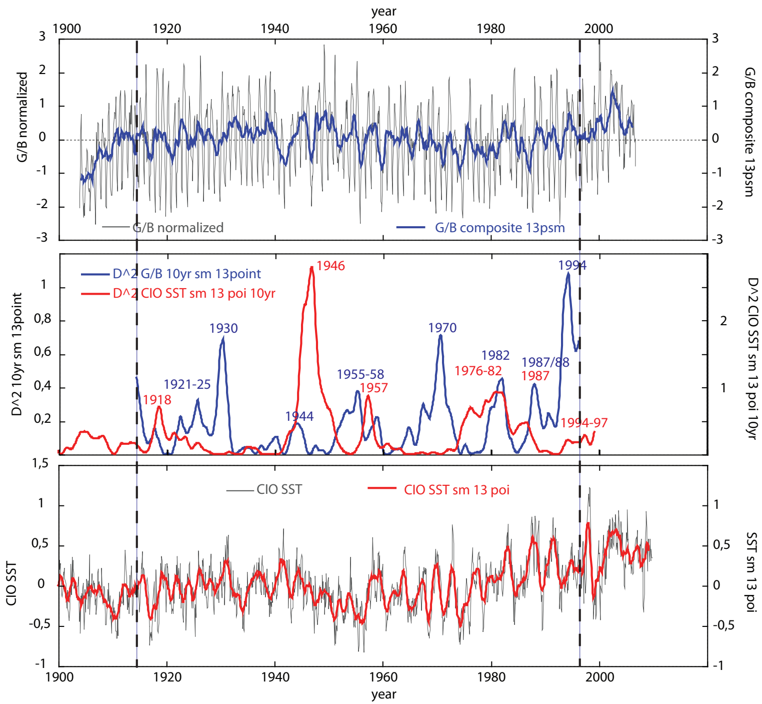

Fig. C2. Record segmentation of the south CIO ERSST (Smith et al., 2008) vs. 3 core composite G/B (MAS1, MAS3 and ANDRA). The top panel shows the raw G/B record with a 13 point smoothing superimposed. Middle Panel shows the change points which are above the 95 % significance level. Major change points are indicated by years (red = CIO SST; blue = G/B). Lower panel shows the raw CIO SST time series with a 13 point smoothing superimposed. The vertical dashed line marks the start and end point for reliable interpretation of the record segmentation analysis taking into account that the first and last 10 yr cannot be used for interpretation.

CPD

8, 787–817, 2012

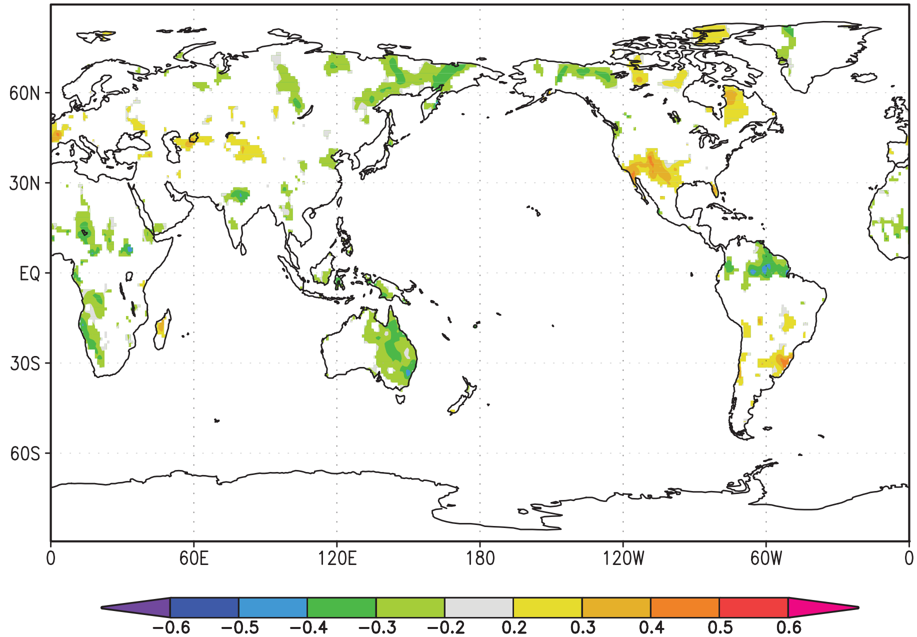

Fig. D1. Spatial correlation of mean annual averages (May to April) of the Pacific Decadal Oscillation (PDO) (Mantua et al., 1997) with global annually averaged (May to April) rainfall data produced by the Climate Research Unit (CRU) at the University of East Anglia (CRU TS3) (Mitchell and Jones, 2005). Colour shading represents confidence of 90 % and greater. Red shading indicates positive correlations and green negative correlations. Note the positive correlation of rainfall with the PDO over Madagascar and negative correlation over Eastern Australia and the Northern Rocky Mountains. Correlations were computed at http://climexp.knmi.nl/.

CPD
8, 787–817, 2012